

Ultrasonic tomography in concrete

Tomografia ultrassônica em concreto

L. P. PERLIN ^a
lourencopp@gmail.com

R. C. A. PINTO ^b
rpinto@ecv.ufsc.br

Abstract

The application of the ultrasonic pulse velocity method for internal flaw identification in concrete members has been gaining importance in the last years. This non destructive method has benefits, but also presents some limitations, especially in the field of representation of the results. The goal of this paper is to improve the representation of the results with the application of the computational tomography technique. This technique allows to better locate internal flaws by a tomographic image called tomogram. A tomogram exhibits flaw position within the sectional planes of the analyzed concrete members. International researchers agree that the ultrasonic tomography technique has great potential to be used in the investigation of internal sections of concrete members as well as to identify internal flaws. The experiments performed in this work endorse this statement.

Keywords: nondestructive test, ultrasonic, tomography.

Resumo

O método ultrassônico convencional para a detecção de não homogeneidades no concreto já é conhecido no meio acadêmico e está em expansão na área técnica. Tal método tem suas vantagens e limitações com relação à representação dos resultados obtidos. Esta pesquisa, nacionalmente pioneira, visa melhorar consideravelmente tais resultados com a aplicação da técnica tomográfica computacional, cujas localizações das não homogeneidades são proporcionadas por tomogramas, onde é possível conhecer suas posições dentro de planos seccionais do elemento de concreto sem armadura analisado. Pesquisadores internacionais afirmam que a técnica da tomografia ultrassônica em concreto tem grandes potencialidades para ser utilizada na investigação de seções internas de concreto para identificação de não homogeneidades. Através de ensaios experimentais, os resultados dessa pesquisa reafirmam tal constatação.

Palavras-chave: ensaios não destrutivos, ultrassom, tomografia.

^a Universidade Federal de Santa Catarina, Departamento de Engenharia Civil, lourencopp@gmail.com, Campus Universitário Reitor João David Ferreira Lima - Trindade - Florianópolis - Santa Catarina – Brasil - CEP 88040-970. Doutorando em Engenharia Civil, área Estruturas.

^b Universidade Federal de Santa Catarina, Departamento de Engenharia Civil, rpinto@ecv.ufsc.br, Campus Universitário Reitor João David Ferreira Lima - Trindade - Florianópolis - Santa Catarina – Brasil – CEP 88040-970. Professor Associado do curso de Engenharia Civil.

1. Introduction

Some time ago concrete structures were believed to last eternally, i.e., not being subjected to deterioration. Nowadays, however, it is known that such structures may suffer degradation effects with time. There are several examples of highway structures all over the world that need to be repaired. The nondestructive tests help to gather information about structure integrity, evaluating the need to corrective actions, as well as contributing to determine the level of intervention needed in the structural element.

Among the various nondestructive test methods available, the ultrasonic pulse velocity method has been widely used in concrete structures. It has been applied to evaluate the resistance of concrete using pre-determined correlation curves between ultrasound pulse velocity and compressive strength (EVANGELISTA [1]; LORENZI [2]; MACHADO [3]; STEIL *et al.* [4]; CÂMERA, E. *et al.* [5]). Ultrasound has also been used to inspect structural elements for the presence of regions with non homogeneities (DORNELLES *et al.* [6]; BUTTCHEVITZ *et al.* [7]; JUNIOR SOARES *et al.* [8]; EMANUELLI JUNIOR *et al.* [9-10]; PERLIN [11]). Usually, the inspection technique used to find internal flaws with ultrasound consists of several readings along the structure surface, resulting in a map of travel times of the ultrasonic pulse within the element as shown in Figure 1.

The ultrasonic pulse velocity is then calculated using the distance travelled by the ultrasound pulse as the thickness of the element. Internal flaws are detected by the existence of regions with lower velocities. The graphical representation obtained by this procedure, however, is not efficient since it is an attempt to express a two dimensional section in an only one dimensional figure.

This graphical representation can be improved considerably with the computerized tomography technique withg ultrasound readings as a physical measure, instead of X-rays. This technique is called Ultrasonic Tomography in Concrete. Although already known internationally, there is a lack of basic information about this technique.

2. Tomography

Tomography is a word derived from two Greek words, *tomus* and

grafos which respectively mean “slice” and “image or design”. The history of tomography begins in 1895, when the German physicist Wilhelm Conrad Röntgen produced electromagnetic radiation at wavelengths corresponding to the currently called X-rays. As a consequence, he is considered the “father of radiology.” He earned the Nobel Prize in Physics in 1901 (MARTINS [12]). The images produced by this technique (Figure 2) are projections on a screen, and therefore, represent a three dimensional object on a two dimensional plane. This limitation is similar to the one in conventional ultrasonic tests, since there is also an attempt to represent a two dimensional section by one dimensional figure (Figure 1).

In 1917 the Austrian mathematician Johann Radon presented a solution of this problem. He showed that it is possible to exactly reconstruct a three dimensional object from a complete set of its two dimensional projections, each obtained at a specific angle. This technique is considered the mathematical basis for computerized tomography, being called the Radon Transform (DEANS [14]; IUSEM *et al.* [15-16]).

Despite being mathematically possible, it was very laborous to perform a tomography without the aid of a computer or automatic equipments. Therefore, in 1972, the first computerized tomography equipment was developed by the English electrical engineer, Godfrey Newbold Hounsfield, and by the South African physicist Allan MacLeod Cormack. For their accomplishments, they came to receive the Nobel Prize in Physiology and Medicine in 1979 (FILLER [17]).

3. Ultrasonic tomography in concrete

The computational tools available nowadays, together with the mathematical techniques developed by Radon, help to develop the computerized tomography in concrete. The ultrasonic pulse velocity is used as the physical measure.

3.1 Basic mathematical background

The ultrasonic pulse velocity between two transducers can be obtained from Equation 1. Since the positions of the transducers are known, the total travel distance L can be determined. The results

Figure 1 – Conventional ultrasonic method for internal flaws searching

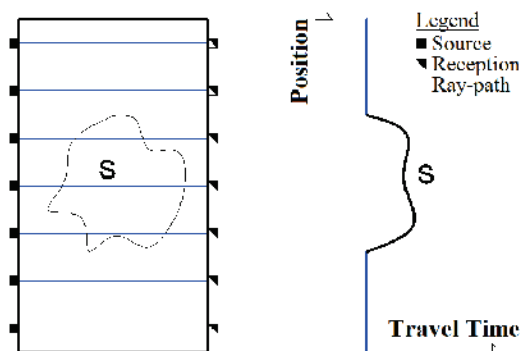


Figure 2 – First X-ray image (Haase (13))



of the ultrasound reading is the total travel-time T of the ultrasound wave, thus the ultrasound velocity is automatically known (MALHOTRA *et al.* [18]).

$$V = \frac{L}{T} \quad \therefore T = \frac{L}{V} \tag{1}$$

One could divide the section to be analyzed in a grid of n elements (Figure 3-b) in that case the ultrasonic pulse travels through several elements at known distances. The total travel path L is the sum of all distances travelled in each element. Similarly, the sum of the individual time to travel each element is the total travel-time T . Therefore, the total travel-time T could be determined as presented in Equation 2.

$$T = \int_E^R \frac{1}{V_j} * dL_j \tag{2}$$

where:

T : total travel-time of the ultrasound wave from the transmitter to the receiver;

V_j : ultrasound velocity in element j ;

dL_j : travel distance in element j .

Equation 2 could be rewritten considering the term wave slowness (p) as the inverse of wave velocity, as expressed in Equation 3 (JACKSON *et al.* [19]).

$$T = \int_E^R p_j * dL_j \tag{3}$$

where:

P_j : wave slowness in element j .

Equation 3 could also be regarded as a summation, as shown in Equation 4, where n is the total elements.

$$T = \sum_{j=1}^n p_j * dL_j \tag{4}$$

Each ultrasound reading can be expressed by Equation 4. The total number of ultrasound readings (m) is represented in Equation 5, which is graphically represented in Figure 3-c.

$$T_i = \sum_{j=1}^n p_j * dL_{i,j} \quad (i=1, \dots, m) \tag{5}$$

Equation 5 could be expressed in matricial form according to Equation 6.

$$\underline{T}_m = \underline{D}_{m,n} * \underline{P}_n \tag{6}$$

where:

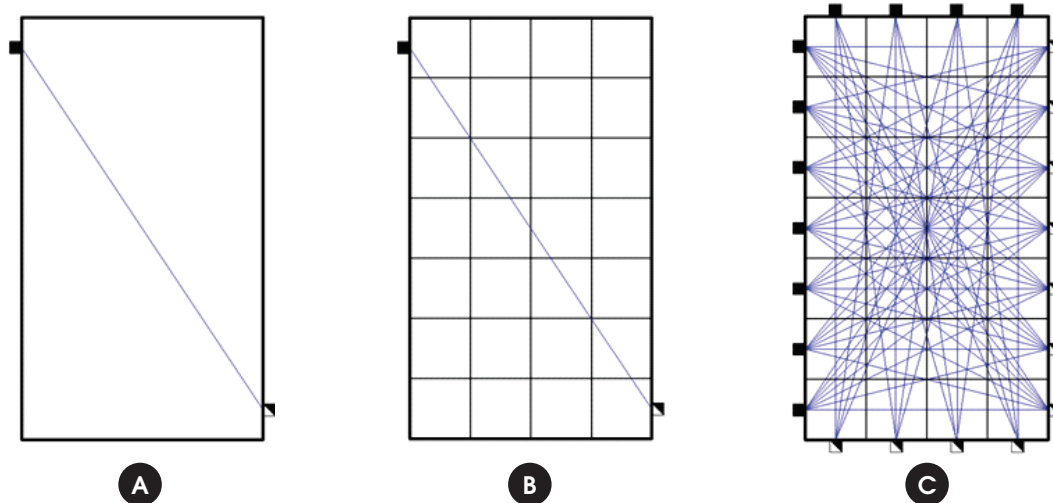
m : total number of ultrasound readings;

n : total number of elements;

D : a rectangular matrix with m lines and n columns that records the travel distances of the ultrasound waves in element j , when reading i is performed;

P : a column vector with n lines that records the wave slowness in each different element j ;

Figura 3 – Representação das leituras ultrassônicas – (a) leitura – (b) leitura com elementos discretizados – (c) várias leituras com elementos discretizados



T: a column vector with m lines that records the total travel-time of each reading i .

It can be observed that the elements of matrix D are determined since the grid and the position of the transducers are known for each different reading. The elements of vector T are also known since they are the results of each reading. Therefore, only the elements of vector P are to be determined.

3.2 Resolution

Equation 6 represents a system of simultaneous linear equations, which could apparently be solved by simplified methods. However, the matrix D is usually rectangular, with a number of equations that differs from the number of the unknowns wave slowness. Moreover, there are some equations that are linearly dependent, which may lead to a singular problem, without a unique solution.

Therefore, depending on the number of readings and on which readings are performed, the problem may be:

■ **underdetermined**: the number of linearly independent equations

is less than the number of unknowns, and thus there is not a unique solution (Figure 4-a);

■ **determined**: the number of independent linearly equations is equal to the number of unknowns, and thus there is a unique solution (Figure 4-b);

■ **overdetermined**: the number of independent linearly equations is greater than the number of unknowns. If the readings are accurate, the system will be considered **consistent** with a unique solution (Figure 4-c). If, on the other hand, the readings are not accurate, the system will be **inconsistent** without a proper solution to all readings (Figure 4-d).

The tomographic system can be classified as underdetermined, determined or overdetermined depending on the concrete element to be study and its number of available sides to perform ultrasound readings. For beams and slabs, there are usually only two sides available, according to Figure 5-a. For columns, there are usually four sides that can be used, which allow the readings to be as shown in Figure 5-b. It may be necessary to use different modes of readings depending on how the objects are on the field Perlin [11].

Figure 4 - Classification of the simultaneous linear equations system - (a) underdetermined (b) determined - (c) overdetermined consistent - (d) overdetermined inconsistent

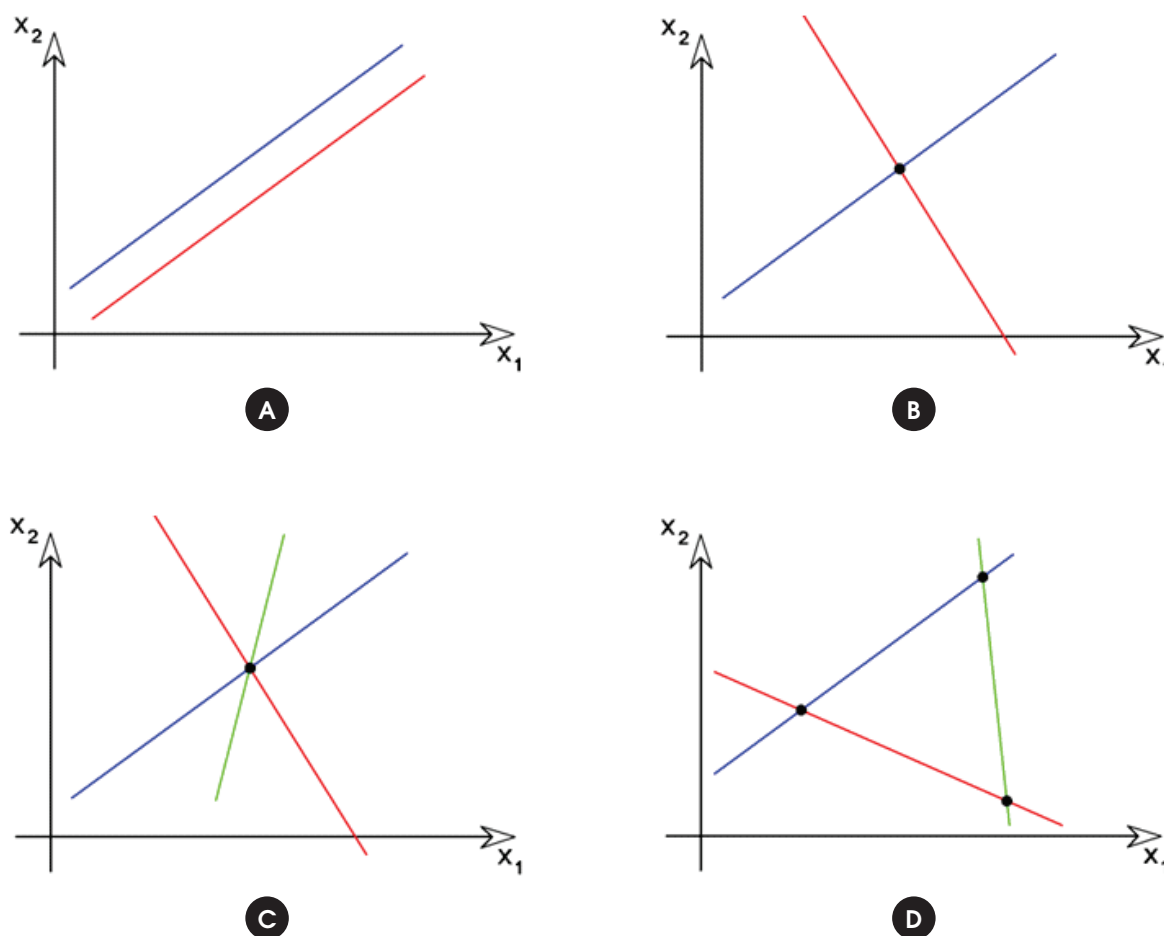
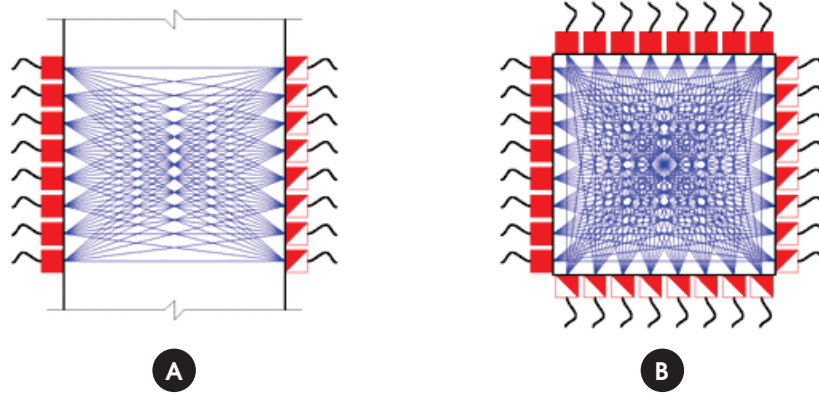


Figure 5 – Modes of measurement – (a) simple opposite faces – (b) complete opposite faces



If the readings are performed only on opposite sides of the concrete element, the simultaneous system of equations is undetermined, regardless the number of readings performed (JACKSON *et al.* [19]). If the readings are performed on all four opposite sides, the simultaneous system of equations is overdetermined; for actual readings with intrinsic errors associated with, this system may be inconsistent (Figure 4-d). The underdetermined simultaneous system of equations is beyond the scope of this paper. Hereafter, only the determined and the overtermined systems are discussed. Among the methods used to solve the simultaneous system of linear equations, there are direct and iterative methods. The direct methods used are: solution by the inversion of matrix D, Cramer's Rule, Gaussian Elimination, and the Minimum Least Squares Method. On the other hand, the iterative methods are Gauss-Jacobi, Gauss-Seidel, Kaczmarz and Cimmino methods. According to Perlin [11], the best method to be used in the rectangular simultaneous linear equation system characteristic of a tomographic process is the Cimmino iterative method. Jackson *et al.* [19] presented an improvement of this method allowing to a faster convergence. This optimized modification of Cimmino method is called optimized Cimmino, and is presented in Equation 7.

$$\underline{P}_n^{(k)} = \underline{P}_n^{(k-1)} + \underline{W}_{m,n}^T * [\underline{T}_m - \underline{D}_{m,n} * \underline{P}_n^{(k-1)}] \quad (7)$$

where:

k: current iteration number;

m: number of simultaneous equations;

n: number of unknowns;

$\underline{P}_n^{(k)}$: column vector that stores the values of current iterative step ;

$\underline{P}_n^{(k-1)}$: column vector that stores the values of previous iterative step;

$\underline{W}_{m,n}$: matrix given by:

$$w_{ij} = \frac{d_{ij}}{N_j * \sum_{k=1}^m (d_{ik})^2} ; \quad (8)$$

N_j : number of equations where j is not zero;

d_{ij} : value of row i and column j of the matrix $\underline{D}_{m,n}$.

In order to better understand the solution process of the tomographic problem, one should identify that the term inside brackets represents the variation $\underline{DT}_m^{(k)}$ of the iteration pass k. While performing the first iteration is necessary to define an initial value for $\underline{P}_n^{(0)}$. The transposed matrix $\underline{W}_{m,n}$ calculates the variation of the ultrasound pulse velocities of each element due to the variation of time readings $\underline{DT}_m^{(k)}$, yielding $\underline{DP}_n^{(k)}$ for iteration k. $\underline{DP}_n^{(k)}$ is then added to $\underline{P}_n^{(k-1)}$, resulting in the best possible velocity field.

In order to solve the proposed problem it is mandatory to use a tomographic software. In this research, it was decided to develop and continuously optimize a computational program, called TUCon, which comes from Ultrasonic Tomography in Concrete.

Since object dimensions are known, the grid used and the ultrasound readings performed follow a reference nomenclature according to Figure 6. TUCon calculates the path of each pulse through each element, and thus is able to build the matrix $\underline{D}_{m,n}$. Besides, since the ultrasound readings are known, TUCon builds the vector \underline{T}_m , which represents the travel times.

Figure 6 – Measurement points for two dimensional case

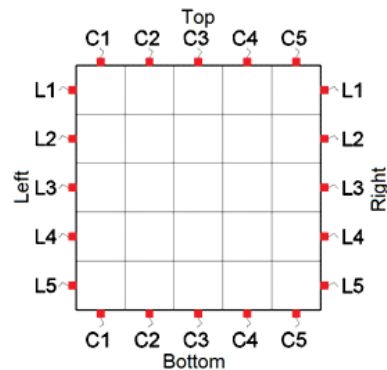
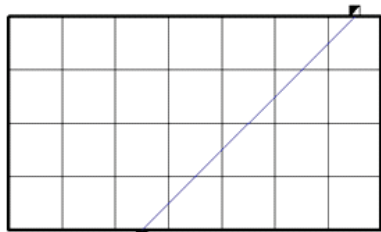


Figure 7 – Pulse travels through different discretized elements

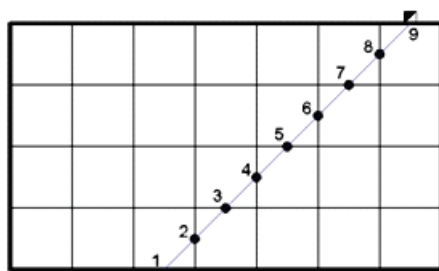


For each reading performed, there is a specific spatial position of the emitting and of the receiving transducers. Initially, it was considered that the pulse travels in a linear path between both transducers, and thus, the mathematical line equation between transducers is defined, according to Figure 7. The real path of the pulse, however, may contour objects or regions with low velocities, as shown in Jackson *et al.* [19]. In this case, a more complex approach needs to be used when programming. This complexity is not yet included in TUCon in its actual phase.

Some aspects should be taken into account when defining the grid to be used in ultrasonic tomography. From a pure mathematical point of view, the Radon Transform does not define limits to the lowest element size to be used, and thus the lowest grid spacing. A great number of elements would allow a more precise result since the domain would be discretized in yet smaller elements. The number of reading points and the total number of readings would also be greater which would contribute to a better result. The possibility of infinitesimal grid spacing would yield theoretically a perfect result.

However, according to results presented by Schechter *et al* [20], the wave front is not perfectly circular, depending mainly on the size of the transducer used to generate it. Therefore, small variations in the transducer position would not influence significantly on the ultrasound readings. Other limiting factors are the wave length

Figure 8 – Pulse travels through different discretized elements with numbering of the intersection points



and the total time required to perform all readings. If an internal flaw is smaller than the wave length it will not be detectable, and thus there is no need to define grid spacing smaller than the generated wave length. Moreover, the smaller the grid spacing the greater the number of readings leading to a much greater execution time for all readings. As a consequence, the decision of the grid spacing should take into account all of this aforementioned factors. The elements of matrix $D_{m,n}$ are calculated following a simple procedure. With the grid spacing and ray-path equation defined, it is possible to determine the interception points, numbering them in an ascending order according to Figure 8. With the points numbered, the distance between successive points can be easily calculated.

With the matrix $D_{m,n}$ and the vector T_m determined, the iterative process of Optimized Cimmino solves the system. The result is then exported for further graphical treatment. The flowchart of the program can be found in Figure 9. The TUCon main window is displayed in Figure 10.

4. Experimental program

4.1 Description of experimental program

Four 20 cm cubic specimens were produced in the laboratory. Inside each specimen, a small EPS block was inserted prior to concreting. Figure 11 shows the geometry of the produced cubes with the position and dimension of the EPS blocks. Metallic molds were used in order to obtain surfaces without irregularities, improving the ultrasound readings. The process of concreting and preparation of specimens is shown in Figure 12.

Once demolded, the specimens were wrapped with plastic film for 10 days. A 5 cm grid spacing mesh (Figure 12-d) was chosen as reference for transducer position. Each specimen was tested using 200 kHz ultrasound transducers.

4.2 Ultrasound readings

The experiments were performed in a two-dimensional plane, using a 2.5 cm spacing grid at the horizontal median plane of the specimens. This allowed performing an ultrasonic tomography at mid-height of the cube exactly at the middle of the internal flaw produced by the EPS. This configuration is similar to a possible

Figure 9 – Flowchart of use and processing of TUCon

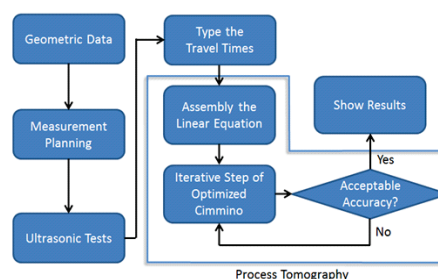
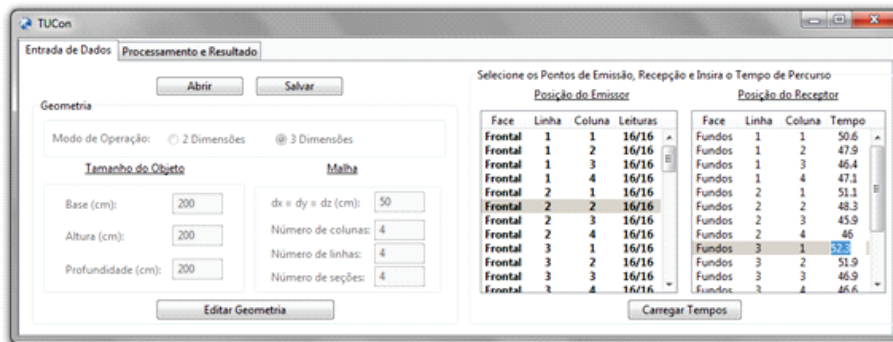


Figure 10 – Main window of the tomography software TUCon



use in a linear element, for example, a column. Figure 13 shows the transducers positions. The 2.5 spacing grid yielded eighth reading points per cube side. As a consequence, a total of 128

readings were performed in each cube, with a total of 512 readings for all specimens. The recommendation of a minimum distance of the transducers to

Figure 11 – Concrete specimens with diferentes EPS blocks inside

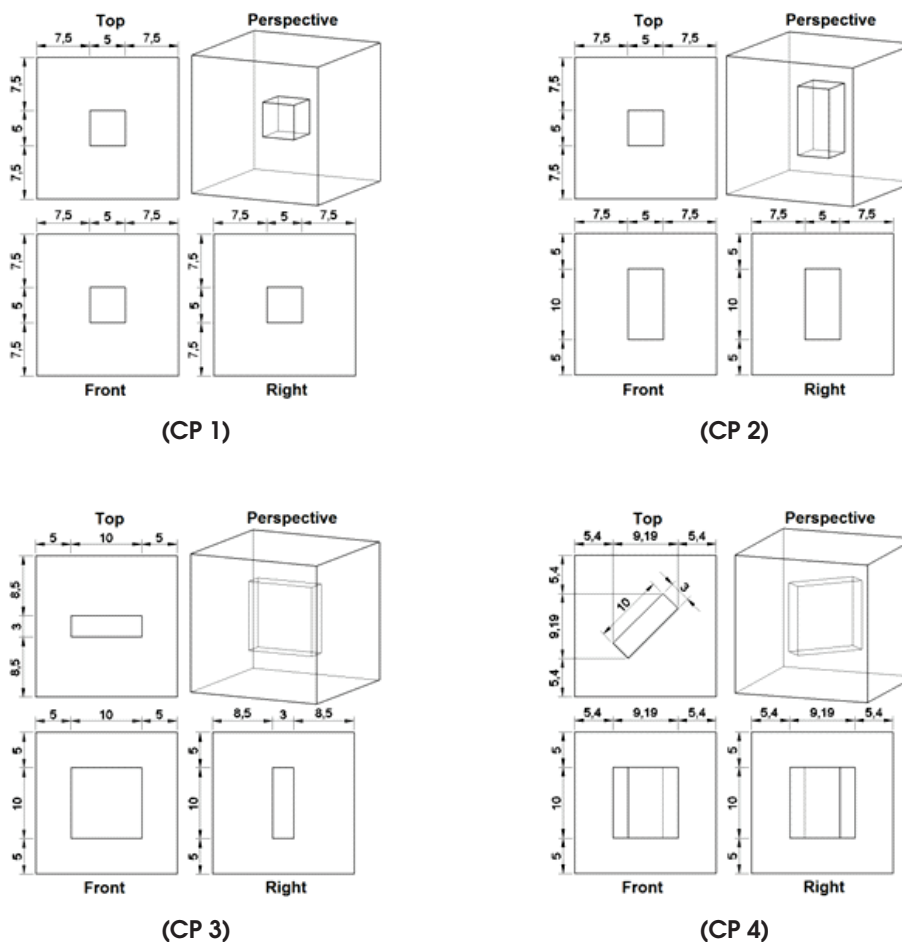


Figure 12 – Production of specimens – (a,b) concreting – (c) demolding – (d) grid spacing



the edges of the object (MALHOTRA *et al.* [18]) was approximately 2.25 cm for the specimens tested here. Such a recommendation was not followed, because if the readings at the edges were not executed, the system of equations would be underdetermined (Figure 4-a), making it impossible to obtain a single solution. Thus, it was already expected that the readings taken at the edges of

specimens might suffer some interference that could reflect in the resulting tomograms.

4.3 Results

After the experimental program has been concluded, the geometry,

Figure 13 – Positioning of 200 kHz transducers – (a) location of the measuring points (b) measurements in analysed section

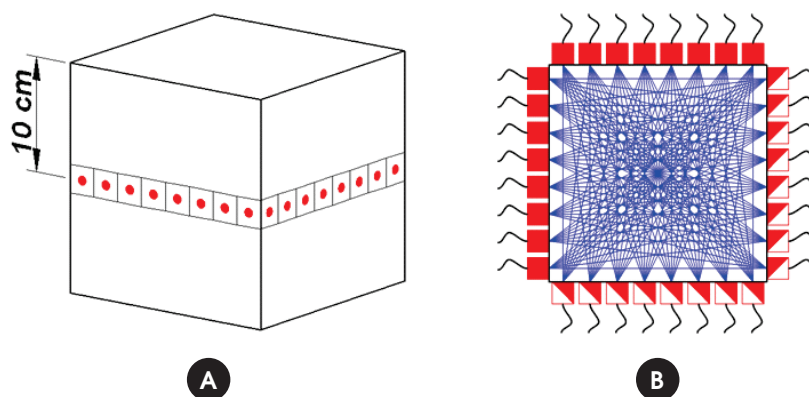
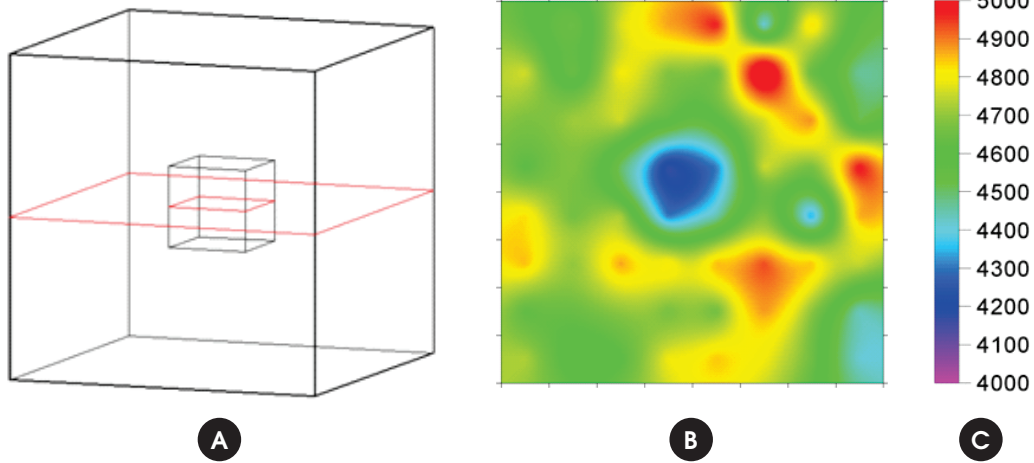


Figure 14 – CP1 Tomogram – (a) specimen and location of analysed section
(b) tomogram – (c) legend in m/s



the grid spacing, and the travels time for each specimen were introduced in TUCon. TUCon, then, processed and exhibited the numerical results. These results were exported and inserted into another third-party program to generate, by linear interpolation, the tomograms shown, in Figure 14 to 17, representing sections at mid-height of specimens CP1, CP2, CP3 and CP4, respectively.

4.4 Analysis of results

The tomogram of CP1 specimen (Figure 14) showed good reconstruction of the analyzed section. It is clear that the 5 cm EPS block is at the center of the section with its correct size. In tomo-

gram of Figure 14, as well as in the others produced, there is some variation on the ultrasonic velocity in regions without internal flaws, represented by the colors yellow to red. This variation does not invalidate the results, since it should be considered that in an actual experiment, the material is not homogeneous and thus the readings can bring small inaccuracies. These variations would tend to decrease if smaller grid spacings were used.

The tomogram of CP2 specimen (Figure 15) presents a similar shape to Figure 14 but with lower ultrasound velocities, represented by the violet regions. Since the only difference between CP1 and CP2 is the height of the EPS block inserted into the specimens (5 cm to 10 cm for CP1 and CP2, respectively), it can be assumed

Figure 15 – CP2 Tomogram– (a) specimen and location of analysed section
(b) tomogram – (c) legend in m/s

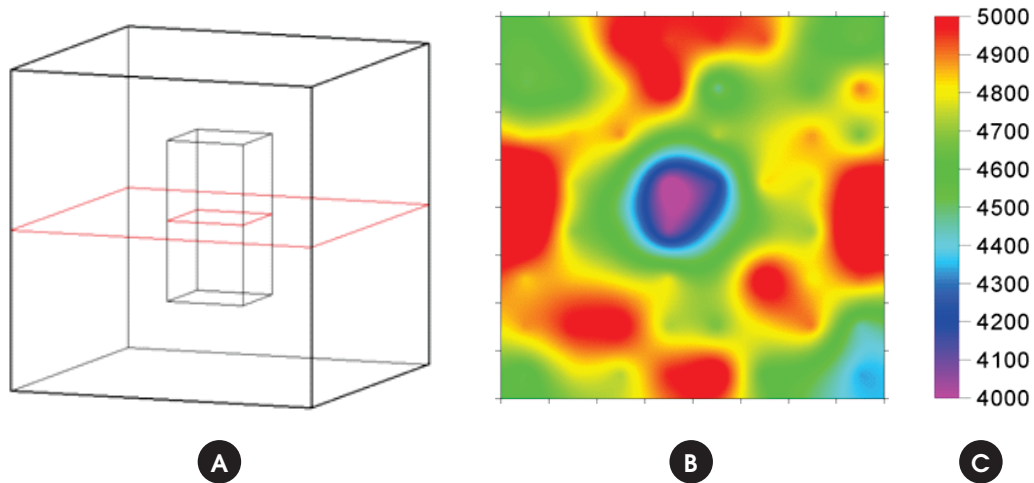
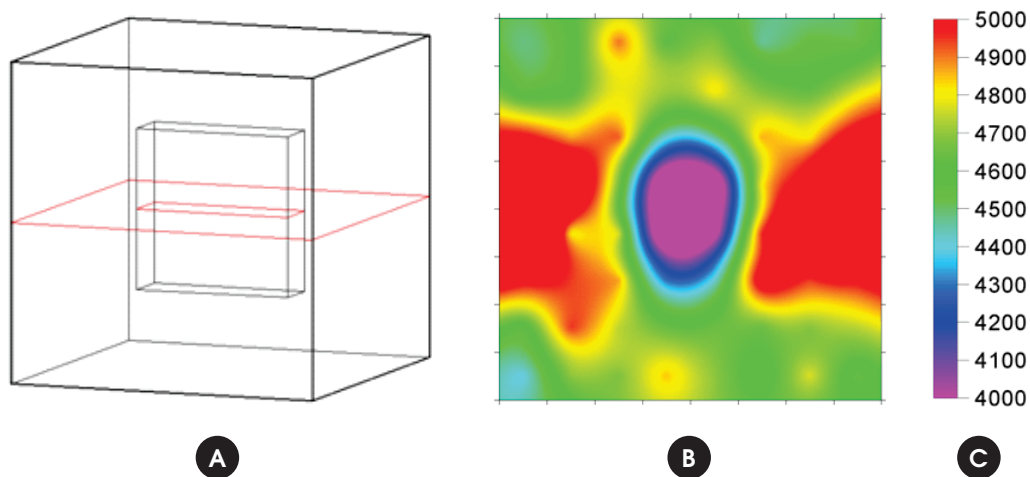


**Figure 16 – CP3 Tomogram- (a) specimen and location of analysed section
(b) tomogram – (c) legend in m/s**



that the EPS size is the cause of such changes in the tomograms. The ray-paths in CP1 probably travel not only surrounding the sides of the EPS block, but also above and below it, depending on the reading. This does not occur in the readings performed on CP2. As an example, in CP1, the estimated travel length of the wave propagation surrounding the EPS block at its top face is 25.6 cm while the same length through the lateral side is 25.9 cm, as shown in Figure 18-a. Thus, the faster ray-path passes through the top face of the EPS block.

On the other hand, the height of EPS block in specimen CP2 prevents the faster ray-paths to travel through the top side of the EPS block since the total distance for this route is 27.5 cm while the

distance through the EPS side is 25.9 cm (Figure 18-b). This difference between the EPS blocks of CP1 and CP2 generates larger ray-path to readings in CP2, explaining the observed stronger violet region in tomogram of Figure 15, when compared with the tomogram of Figure 14.

The tomogram of CP3 specimen (Figure 16) shows an oval shape low velocity region, with the greatest dimension perpendicular to the EPS block inserted. The ultrasound readings that pass through the center of EPS are the most affected by its rectangularity. Therefore, these readings yield slower velocities; the tomography process takes this slowness to the grid elements at the center of the EPS and to perpendicular regions nearby. This effect is called

**Figure 17 – CP4 Tomogram – (a) specimen and location of analysed section
(b) tomogram – (c) legend in m/s**

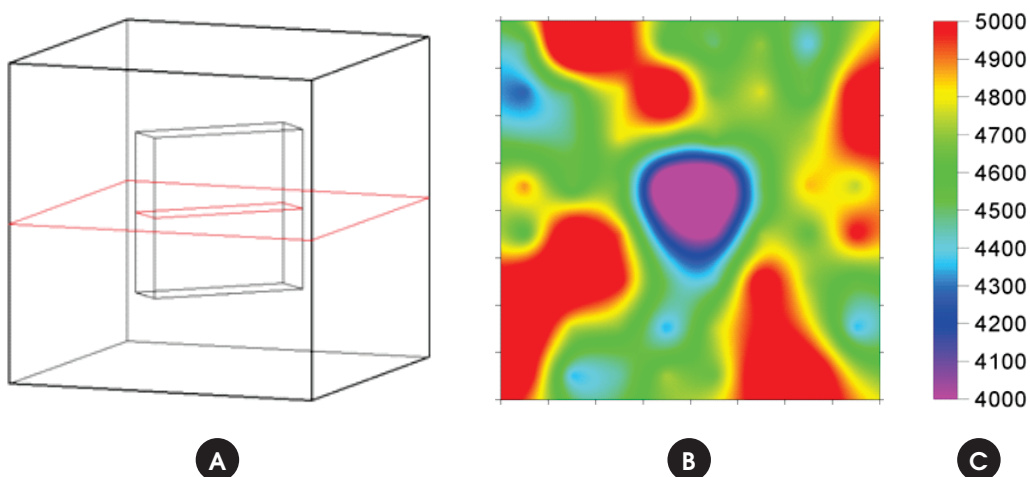
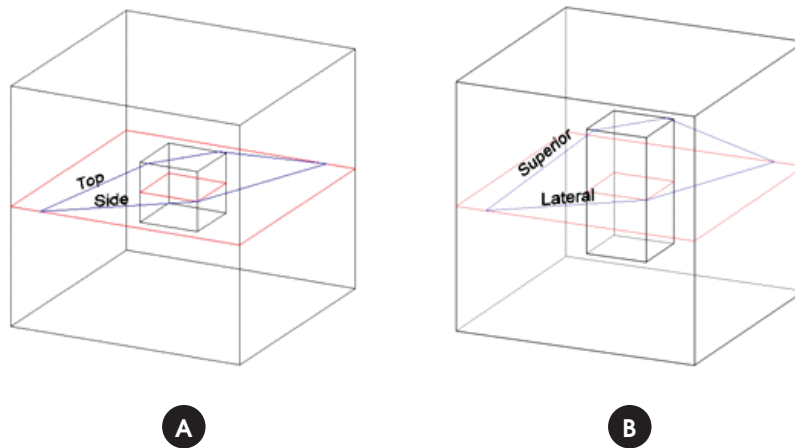


Figure 18 – Possible ray-paths of ultrasound pulses within the specimen – (a) CP1 – (b) CP2



wall effect. It only occurs because it is considered that ultrasonic pulses travel in linear path between the transducers.

The tomogram of CP4 specimen (Figure 17) shows a similar behavior to the one for CP3 specimen (Figure 16), with wall effect also present in CP4, but overlapped in the vertical and horizontal directions. As noted, this provides more circular shape for the violet area in the tomogram.

5. Conclusions

As a result of this research, it can be concluded that the tomographic software TUCon is able to assemble and to solve the tomographic problem, having been validated from experimental data. The two-dimensional tomograms produced by ultrasound readings with 200 kHz transducers were able to well represent the analyzed sections of the specimens. The tomograms for CP3 and CP4 specimens exhibited some irregularities, suggesting an oval or circular shape for a rectangular internal flaw. This effect was called wall effect. It happened due to the consideration of linear ray-paths between transducers.

The wall effect can be minimized by introducing an algorithm inside the tomographic processing that would calculate the real ray-path, avoiding objects or regions of low velocity. Jackson *et al.* [19] proposed a method to make this consideration. The implementation of this routine is already being developed and should be included in future versions of the software TUCon.

This work also demonstrated the great potential for the utilization of ultrasonic tomography in the nondestructive evaluation of concrete structures. It is expected that this line of research will help to diffuse this knowledge in the academic and technical fields.

6. Acknowledgment

The authors would like to express their gratitude to CNPq, to the Research Group on Nondestructive Testing – GPEND of the Federal University of Santa Catarina, and to Professor Ivo Padaratz by providing resources, equipment and physical space for this work.

7. References

- [01] EVANGELISTA, A. C. J. Avaliação da resistência do concreto usando diferentes ensaios não destrutivos. Tese (Doutorado em Engenharia Civil) – Universidade Federal do Rio de Janeiro, Rio de Janeiro, 2002.
- [02] LORENZI, A. Aplicação de redes neurais artificiais para estimativa da resistência à compressão do concreto a partir da velocidade de propagação do pulso ultra-sônico. Tese (Doutorado em Engenharia Civil) – Universidade Federal do Rio Grande do Sul, Porto Alegre, 2009.
- [03] MACHADO, M. D. Curvas de correlação para caracterizar concretos usados no Rio de Janeiro por meio de ensaios não destrutivos. Dissertação (Mestrado em Engenharia Civil) – Universidade Federal do Rio de Janeiro, Rio de Janeiro, 2005.
- [04] STEIL, R. O. et al. Aplicabilidade de ensaios não destrutivos em estruturas de concreto: um estudo de caso. In: 43° CONGRESSO BRASILEIRO DE CONCRETO, 2001, Foz do Iguaçu. Anais. Foz do Iguaçu: IBRACON, 2001. 1 CD-ROM.
- [05] CÂMARA, E.; PINTO, R. C. de A. Avaliação da resistência à compressão do concreto in loco através de ensaios não destrutivos. In: 48° CONGRESSO BRASILEIRO DE CONCRETO, 2006, Rio de Janeiro. Anais. Rio de Janeiro: IBRACON, 2006. 1 CD-ROM.
- [06] DORNELLES, F. L.; PINTO, R. C. de A.; PADARATZ, I. J. Detecção de falhas internas de concretagem através do uso do ultra-som. In: 47° CONGRESSO BRASILEIRO DE CONCRETO, 2004, Olinda. Anais. Olinda: IBRACON, 2004. 1 CD-ROM.
- [07] BUTTCHEVITZ, A. W. et al. Análise da influência da qualidade do adensamento na homogeneidade do concreto utilizando ensaio não destrutivo. In: 52° CONGRESSO BRASILEIRO DE CONCRETO,

- 2010, Fortaleza. Anais. Fortaleza: IBRACON, 2010. 1 CD-ROM.
- [08] SOARES JUNIOR, P. C.; PADARATZ, I. J.; PINTO, R. C. de A. Influência da presença de armadura na detecção de falhas internas de concretagem através do uso do ultra-som. In: 48° CONGRESSO BRASILEIRO DE CONCRETO, 2006, Rio de Janeiro. Anais. Rio de Janeiro: IBRACON, 2006. 1 CD-ROM.
- [09] EMANUELLI JUNIOR, A. C. et al. Emprego do ultrassom para detectar a presença de cabos de protensão em estruturas de concreto. In: 52° CONGRESSO BRASILEIRO DE CONCRETO, 2010, Fortaleza. Anais. Fortaleza: IBRACON, 2010. 1 CD-ROM.
- [10] EMANUELLI JUNIOR, A. C.; PADARATZ, I. J.; PINTO, R. C. de A. Emprego do ultrassom, eco-impacto e termografia infravermelha para detectar falhas de injeção em cabos de protensão (pós-tensionados). In: 53° CONGRESSO BRASILEIRO DE CONCRETO, 2011, Florianópolis. Anais. Florianópolis: IBRACON, 2011. 1 CD-ROM.
- [11] PERLIN, L. P. Tomografia ultrassônica em concreto: desenvolvimento de ferramenta computacional. Dissertação (Mestrado em Engenharia Civil) – Universidade Federal de Santa Catarina, Florianópolis, 2011.
- [12] MARTIN, J. et al. Ultrasonic tomography of grouted duct post-tensioned reinforced concrete bridge beams. *NDT&E International*, Oxford, v. 31, p. 107-113, 2001.
- [13] HAASE, A. (Ed.); LANDWEHR G. (Ed.); UMBACH, E. (Ed.). *Röntgen centennial: x-rays in natural and life sciences*. Singapore: World Scientific Publishing, 1997.
- [14] DEANS, S. R. *The Radon transform and some of its applications*. New York: John Wiley & Sons, 1983.
- [15] IUSEM, A. N.; PIERRO A. R. de. Fundamentos matemáticos da tomografia computadorizada: método de transformações. *Revista Matemática Universitária*, São Paulo, n. 11, p. 53-65, 1990a.
- [16] _____. Fundamentos matemáticos da tomografia computadorizada: método de expansão em séries. *Revista Matemática Universitária*, São Paulo, n. 12, p. 57-85, 1990b.
- [17] FILLER, A. G. The history, development and impact of computed imaging in neurological diagnosis and neurosurgery. Disponível em: <<http://dx.doi.org/10.1038/npre.2009.3267.5>>. Acesso em: 5/12/2010.
- [18] MALHOTRA, V. M.; CARINO, N. J. *Handbook on nondestructive testing of concrete*. 2. ed. West Conshohocken: Chemical Rubber Company Press, 2004.
- [19] JACKSON, M. J.; TWEETON, D. R. *MIGRATON - Geophysical tomography using wavefront migration and fuzzy constraints*. Minneapolis: U.S. Bureau of Mines, 1994. Report Investigation 9497.
- [20] SCHECHTER, R. S. et al. Real-Time Parallel Computation and Visualization of Ultrasonic Pulses in Solids. *Science Magazine*, Washington, v. 265, p. 1188-1192, 1994.